Effect of salinity on marine propeller performance

Effect of salinity on marine propeller performance

A M Ghoniem[1], A S Abo Elazm[2], M I Benaya[3] and S A Mohamed[4]

[1]MSc. Student, Military Technical College, Ships and submarines Engineering Department, 11766 Cairo, EGYPT
[2]Professor, Military Technical College, Ships and submarines Engineering Department, 11766 Cairo, EGYPT
[3]Doctor, Military Technical College, Ships and submarines Engineering Department, 11766 Cairo, EGYPT
[4]Doctor, Military Technical College, Ships and submarines Engineering Department, 11766 Cairo, EGYPT

E-mail: adelmohab@mtc.edu.eg

Abstract. In order to analyse problems with fluid flow, computational fluid dynamics is one of the most helpful tools available. This paper presents a numerical simulation of the effect of salinity on a marine propeller of an aircraft carrier in advance of the propeller open water (POW) test. A five-bladed fixed-pitch propeller is analysed using an unstructured mesh in the flow domain (PPTC - VP1304). Solving the RANSE equations describing the flow with a streamlined solver To begin, the accuracy of the numerical model was checked by comparing the results to previously published experimental data on the propeller. The verified model was then used to investigate how salinity impacted propeller performance in open water. The effect of fluctuating salinity was investigated by adjusting the properties of the flow fluid in a computational model. Lower advance ratios are where the effect of salinity, a decrease in efficiency of up to 4%, really shows up. However, it had little to no effect at higher advance ratios.

1. Introduction

Marine screw propellers are the most common form of propulsion for ships. They are available in a wide range of sizes and shapes [1] to accommodate a wide range of loads and levels of performance. The primary purpose of these devices is to generate useful thrust through rotation. Since their inception, marine propellers have undergone extensive refinement. This has resulted in a plethora of novel structures suitable for a wide variety of applications. In the beginning, the model basin test was the only trustworthy means of evaluating propeller efficiency. With the advent of the first empirical models [2], engineers no longer need to conduct a large number of experimental tests to predict the performance characteristics of modified propeller designs. Computational fluid dynamics (CFD) can be used to solve a variety of ship hydrodynamics problems [3] due to its relatively accurate results and shorter computational times compared to experimental approaches. Several computational fluid dynamics (CFD) applications, such as Lifting Line Theories [4], Blade Element-Momentum Theory, Surface Panel Methods, Boundary Element Methods (BEM), and Reynolds Averaged Navier-Stokes Equation (RANSE) [5], utilise various techniques to estimate the characteristics of propellers in open water. A lot of scientests use RANSE because its flow model is so close to the physical reality of flows [6]. However, more time and money are needed for computation. In order to run a successful CFD RANSE simulation, it is essential to choose the right mesh (mesh type, mesh size, and mesh structure) and physics models [7]. Many researchers and writers have speculated on the efficiency of propellers. Propeller open water characteristics were compared using the RANSE method by M. Morgut and E. Nobile [8]. The techniques include a revolving grid, frame of reference, and domain. The calculations were performed using a tetrahedral grid, and the ”SST k-omega” turbulence model with two equations was used for the simulations. In this study, it was found that rotating reference frame is a viable option for open water simulation due to its favourable computational time, accuracy, and convergence of results. Most physical properties of seawater are similar to those of pure water and can be understood as a function of temperature and pressure. In addition to temperature and pressure, salinity (the amount of salt dissolved in water) should be considered a third independent property. Variations in water properties cause a wide range of water types. Seawater is an amalgam of pure water and salt from the ocean. The density of water in oceans and seas affects how well propellers work [9]. Gas solubility in water decreases with increases in temperature and salinity. As salinity increases, water viscosity decreases [10]. Since density is sensitive to all salt constituents, it can be used to detect any variation in composition. The density values

can be converted to salinity with the help of a density-salinity relation. To use such a relation with a target salinity uncertainty comparable to that obtained from conductivity measurements, a density measurement with an uncertainty of 2 gm^3 is required. Computational Fluid Dynamics (CFD) was used to analyse the designed propeller's open water characteristics and the impact of water salinity on its performance in this study.

2. SPECIFICATIONS OF THE SELECTED PROPELLER

Five-bladed propeller with the model number VP1304 (or PPTC) and designed pitch coefficient P0.7/D = 1.635 was the subject of the analysis. In model scale, this is a right-handed adjustable pitch propeller. The scale effects of a conventional propeller were investigated using the controllable pitch propeller VP1304. The SVA Potsdam [11] previously released the VP1304, which was used in the Hamburg-based PPTC (Potsdam Propeller Test Case) propeller workshop that took place during the smp'11 conference. Table compiles the basic propeller geometrical information. 1.

Table 1 Propeller main dimensions [11]

Propeller Diameter	D	250 mm
Mean pitch	P_{mean}	391.9 mm
Area ratio	A_E/A_o	0.779
Skew	Θ_{eff}	18.8°
RAke at r/R = 0.7	$\varepsilon_{0.7}$	-9°

2.1. Numerical setup

2.1.1. Test cases Under the same circumstances as the experiment [11], the open water simulation is run with advance coefficients J that ranges from 0.6 to 1.4 with a step of 0.2 as these values have the highest efficiency values of the propeller. The advance velocity was changed to alter J while the propeller revolution remained fixed at n = 15 rev/sec. The parameters for water (density, viscosity) that were selected matched actual values.(density of water ρ = 998.67 kg/m^3, viscosity of water ν= 1.070.10-6 m^2/s [10]).

3. NUMERICAL ANALYSIS OF PROPELLER

Propeller characteristics and pressure distribution on the blade surfaces have been analysed numerically using computational fluid dynamics. The complex geometry of the propeller, coupled with its rotation and forward movement into the water, creates a turbulent flow around the device [12]. CFD software can incorporate the propeller's rotation thanks to the rotating frame of reference method. These governing equations describe the flow around the propeller. Francesco conducted his analysis using a BEM method based on the assumption of an inviscid flow [13]. In this case, CFD's FVM method is used to simulate the flow's viscosity.

3.1. Governing Equations

The governing equations of the method to be solved are written in the following form:

$$\frac{\partial P}{\partial t} + \frac{\partial(\rho u_i)}{\partial x_i} = 0 \tag{1}$$

where ρ= density, u_i is the velocity component in the i^{th} direction (i=1,2,3). The density is constant in case of incompressible flows.

$$\frac{\partial}{\partial t}(\rho u_i) + \frac{\partial}{\partial x_j}(\rho u_i u_j) = -\frac{\partial p}{\partial x_i} + \frac{\partial \tau_{ij}}{\partial x_j} + \rho g_i + F_i \tag{2}$$

where τ_{ij} is the Reynolds stress tensor given by

$$\tau_{ij} = [\mu(\frac{\partial u_i}{\partial x_j} + \frac{\partial u_j}{\partial x_i})] - \frac{2}{3}\mu\frac{\partial u_l}{\partial x_l}\delta_{ij} \tag{3}$$

where p = static pressure,g_i = gravitational acceleration in the i^{th} direction , F_i = external body forces in the i^{th} direction and δ_{ij} is the Kroneker delta and is equal to unity when i=j; and zero when i $\neq$ j. Including the shear stresses in the turbulent flow, the above momentum equation takes on the Reynolds-averaged form, which is given by:

$$\frac{\partial}{\partial t}(\rho U_i) + \frac{\partial}{\partial x_j}(\rho U_i U_j) = \frac{\partial}{\partial x_j}[\mu(\frac{\partial u_i}{\partial x_j} + \frac{\partial u_j}{\partial x_i}) - \frac{2}{3}\mu\frac{\partial u_l}{\partial x_l})] - \frac{\partial p}{\partial x_i} + \frac{\partial}{\partial x_j}(-\rho u_i u_j) \quad (4)$$

3.2. Domain Specifications

As multiples of the propeller diameter D, the flow past the propeller VP1304 was modelled in a cylindrical domain with the following dimensions: 4D forward, 8D rearward, and 5D in diameter (see Figure 1). These parameters were chosen to guarantee that the outlet pressure would be zero and that the boundary conditions would be met. The inlet flow was thought to be homogeneous.

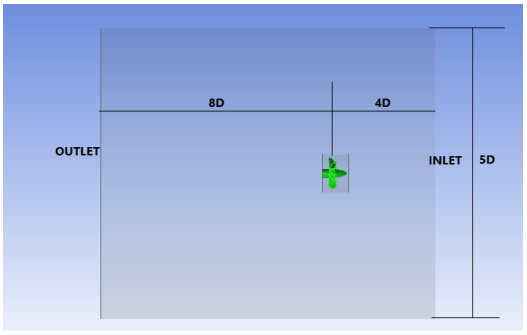

Figure 1 Computational domain geometry

Including a rotating propeller in the simulation and descretizing the flow domain are both challenging aspects of flow over propeller simulation. The domain was characterised by a Tetrahedral Mesh. See figure 2.

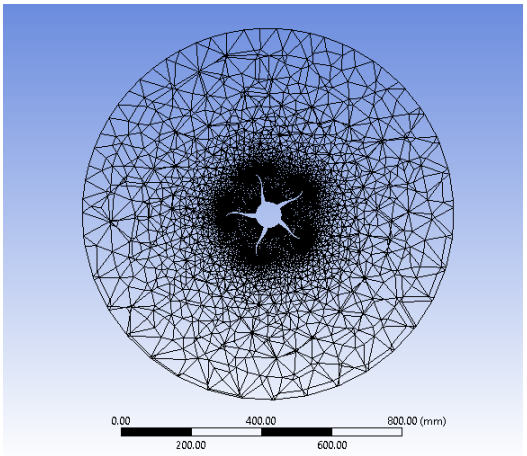

Figure 2 Cross section of the unstructured mesh generated

3.3. Solver Settings

Flow past the propeller was modelled using the Reynolds Averaged Navier-Stokes (RANS) equations and the two-equation "SST k-ω" turbulence model. Using a simpler equation to complete the basic system of Navier-Stokes equations, RANS equations allow for the acquisition of accurate results while keeping calculation times within reasonable bounds in flow . The recommended turbulence model for this type of flow combines the advantages of the basic k-ε and k-ω models [14] and introduces a term that limits the excess kinetic energy of

turbulence in areas of high pressure gradients. The k-ε model successfully predicts the turbulence in the free flow region and demonstrates that the quantities describing the turbulence are robust to changes in the inlet conditions. However, the k-ω model is highly sensitive to values of free-stream turbulence, despite its superior ability to simulate boundary-layer flow. The applied combined model was converted from the k-ε form to the equations for k and ω, and an SST (Shear Stress Transport) term was subsequently introduced. The principal stresses in the flow are constrained by this term. Combining the pressure and velocity fields with the SIMPLE algorithm and an independent solver. Most discretization strategies were second-order methods.

3.3.1. Boundary conditions The given problem is governed by the wall, velocity inlet, and outflow boundary conditions that are imposed on the domain. The velocity inlet boundary condition specifies the inlet velocity and any other relevant scalar properties of the flow. At the inlet, constant velocity profile was adopted perpendicular to the boundary. The outflow boundary condition as the pressure assumed to be atmospheric is used at the outlet. Outflow boundary conditions are used to represent flow exits in cases where the flow's precise velocity and pressure are not known prior to solving the flow problem.

The outflow velocity and pressure are revised in light of a more complete flow assumption. Turbulent fluctuations in the vicinity of the walls are greatly attenuated in any flow because the Reynolds number is very small. The effects of laminar viscosity become more noticeable. In the current setup, slip is allowed close to the lateral surface but only if there is no slip condition on the blade surface itself. With the no slip condition applied to the propeller walls, the drag and lift forces can be calculated. Extraction of thrust from a propeller is possible because lift force is the source of thrust. Even if the boundary is assumed to be 2D away, it does not exist on the lateral surface in a physical flow situation. Since the propeller's behaviour is unaffected by the boundary, this is the case. This is achieved by incorporating a boundary condition based on walls that allows slip near the lateral surface.

Seven different salinity ratios properties were investigated as changing the density and viscosity according to the change in salinity for the values of 0, 20, 40, 60, 80, 100 and 120 g/kg.

3.3.2. VERIFICATION There were three different mesh configurations tested to determine which one provided the best balance of computational efficiency and mesh size as shown in figure 2. For J = 1, a sensitivity analysis of the open water grid was performed. As this ratio is in the middle of the studied range, it was selected as the advance ratio. Created unstructured grids have 0.84x10^6, 4.6x10^6, and 12.9x10^6 elements, respectively. As was to be expected, the smallest grid yields the worst results, with errors close to 4% for the thrust coefficient and 4.5 for torque. As grid sizes grow, there is a direct However, it is impractical to use a grid with 12.9x10^6 cells for a number of CFD analyses, as this is the size at which convergence is steady and where the best overall predictions can be made. Grid with 4.6x10^6 is chosen as the foundation of our study because it offers significant savings in with minimal computational time while offering acceptable results error and because the errors for all cases are low.

Table 2 Mesh study results

Mesh number	K_T error	K_Q error	η_O error
0.84x10^6	6.2%	10.8%	7.6%
4.6x10^6	3.7%	5.1%	3.5%
12.9x10^6	2.2%	3.2%	1.8%

4. RESULTS

In open water, a propeller's performance characteristics typically refer to how its thrust, torque, and efficiency change with forward speed and rotational speed. Experiments are run with models of the propeller that are towed in the towing tank with the revolution rate fixed and the towing speed varied to determine the open water characteristics of the propeller. Open water efficiency is plotted alongside the non-dimensional thrust K_T and the torque K_Q (which is magnified as $10K_Q$ to plot in the same graph). Equations 5-9 are provided for K_T, K_Q, η_O, and J.

$$J = \frac{V_A}{nD} \tag{5}$$

$$K_T = \frac{T}{\rho n^2 D^4} \tag{6}$$

$$K_Q = \frac{T}{\rho n^2 D^5} \tag{7}$$

$$\eta_O = \frac{K_T}{K_Q}\frac{J}{2\pi} \tag{8}$$

Simulation was conducted with the same tetrahedral block unstructured grids for advance ratios ranging from J = 0.6 to J = 1.4, with rotational velocity set at n = 15 s^{-1}. SST k-ω model was adopted for performance assessment in Fluent. The results of simulation were compared with experimental data for the propeller to validate the CFD simulation before investigating the salinity effect. The maximum error was found at the highest advance coefficient for the efficiency as 8.1%. But it was found that the maximum error was 3.6% and 5.7% for torque coefficient and thrust coefficient. see Figure 3

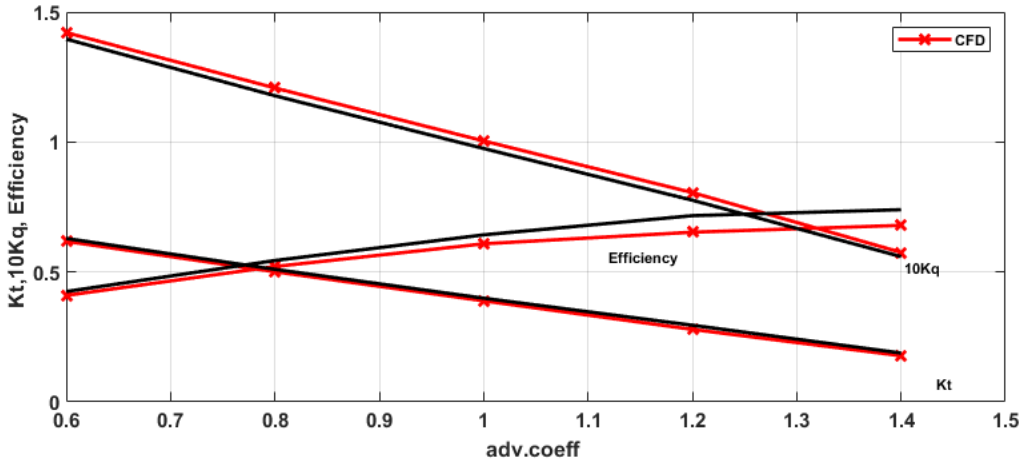

Figure 3 Open Water Characteristics for CFD Model & Experimental

Seven different salinity ratios properties were investigated, as changing the density and viscosity according to the change in salinity was used to determine the water characteristics for each salinity ratio. Inlet velocity was changed in such a way that fairly broad range of advance coefficient is covered.

As shown in Figure 4, at low advance ratios the difference between the thrusts is significant. As the salinity increases, the thrust also increases by average of 4.4% as the water is more denser and the effect of that plays a major role in the hydrodynamic performance of the propeller. For higher advance ratios the effect is less significant and the thrust at all salinity ratios are closer and almost the same.

For the torque analysis as shown in Figure 5, at higher speeds the torque difference between salinity ratios gets smaller. As the salinity increases which increases the density and viscosity by turn the torque required increases as working fluid gets heavier which increases the resistance of rotational motion for the propeller. For an average of 5.4% the torque has increased showing the effect of salinity on the propeller's torque.

As an influence of the change happened to thrust and torque, the efficiency in turn is affected as the salinity increases the efficiency decreases for an average of 0.8%. That is because the increase in torque is higher than the increase in thrust of the propeller. The efficiency gets down as the advance coefficient increases from 0.6 to 1.4. The drop in efficiency reaches 4% for a salinity of 80g/kg and it gets better for higher salinity ratios. The highest efficiency founded to be with lowest salinity ratio 0g/kg, that could be attributed to higher disturbance of flow around propeller due to dissolved particles.

The pressure distribution on the blades differs as the salinity ratio changes, which identify the clearly the response of the propeller's performance due to the salinity change. Figures 7 & 8 show the difference between

pressure contours for the two salinity ratios 0 and 100 g/kg for advance ratio 1.4. The pressure which the propeller is subjected to is higher for the 0 salinity specially on the leading edge.

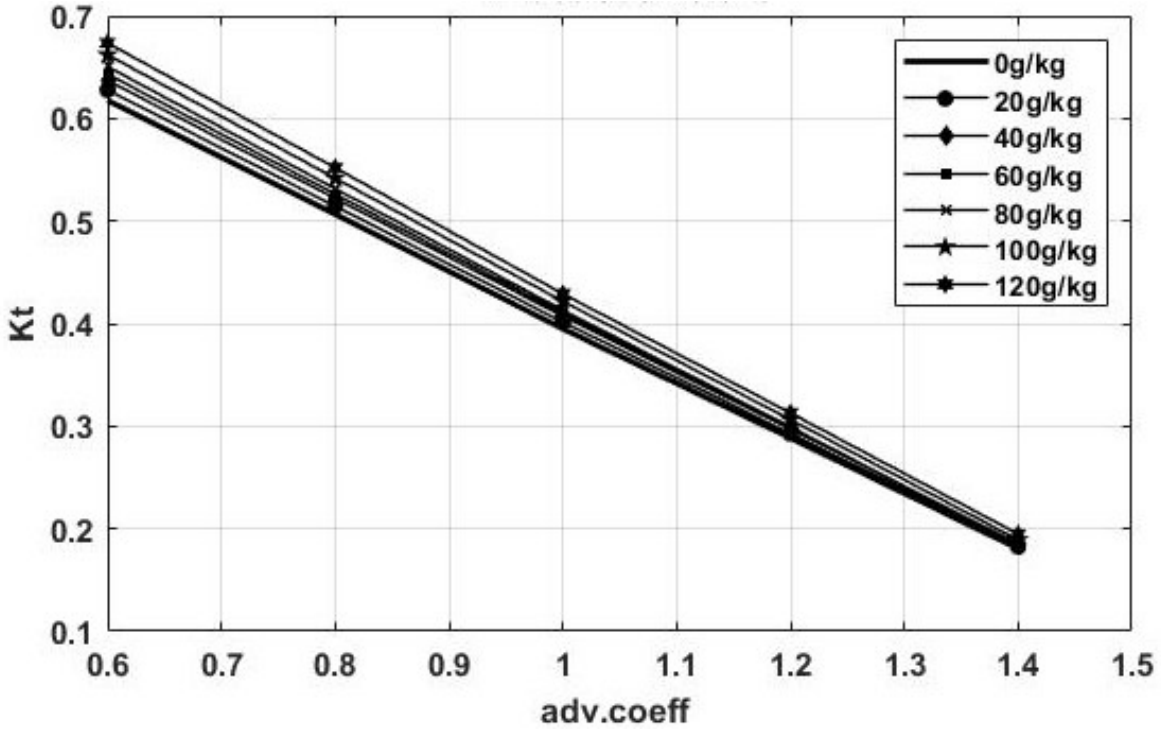

Figure 4 Salinity Effect On Thrust Coefficient

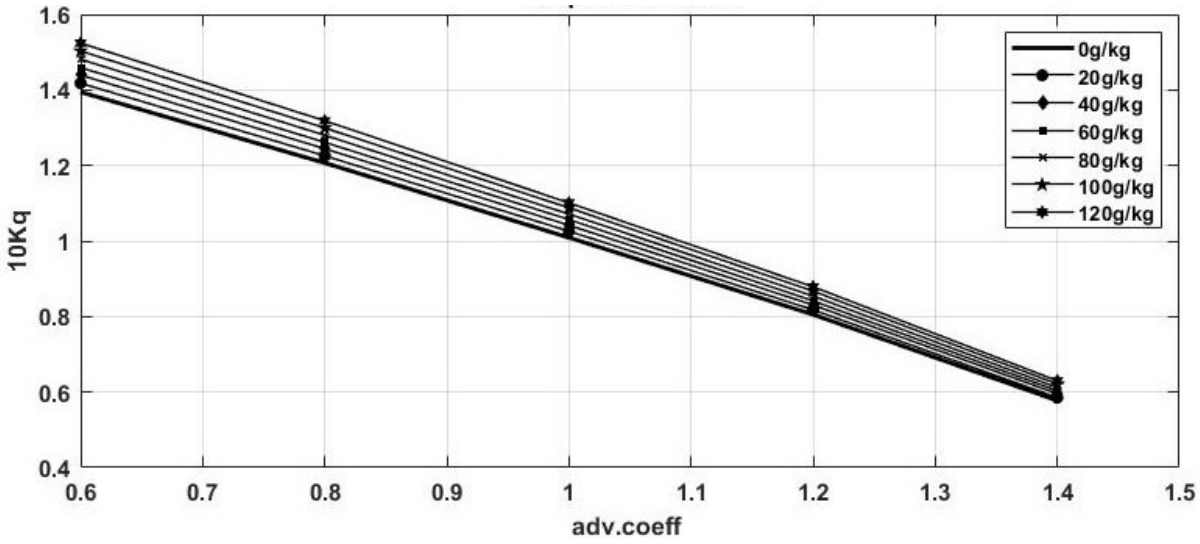

Figure 5 Salinity Effect On Torque Coefficient

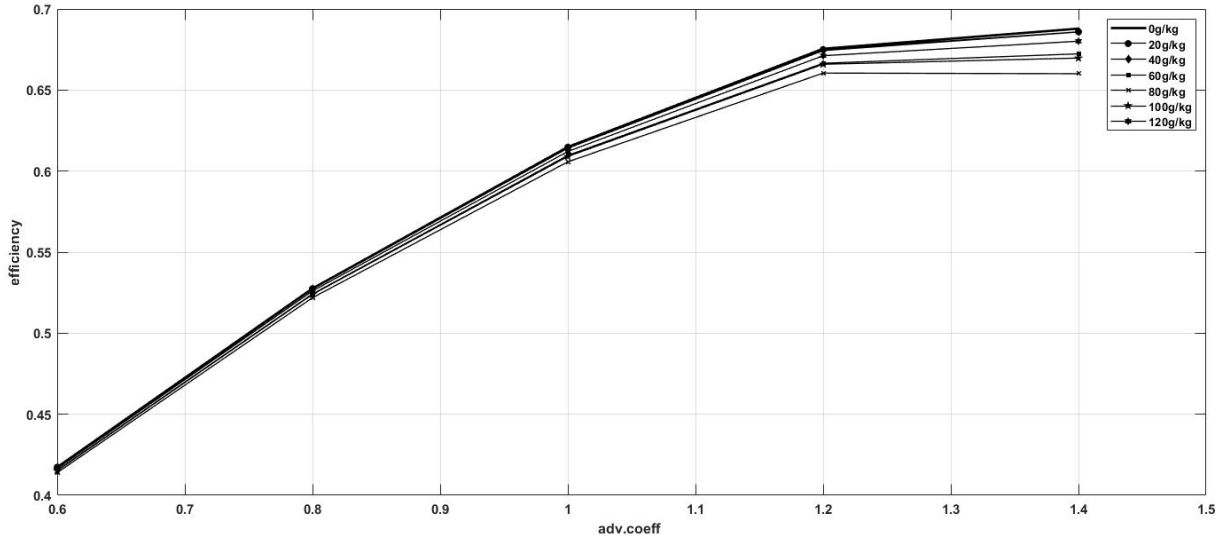

Figure 6 Salinity Effect On Efficiency

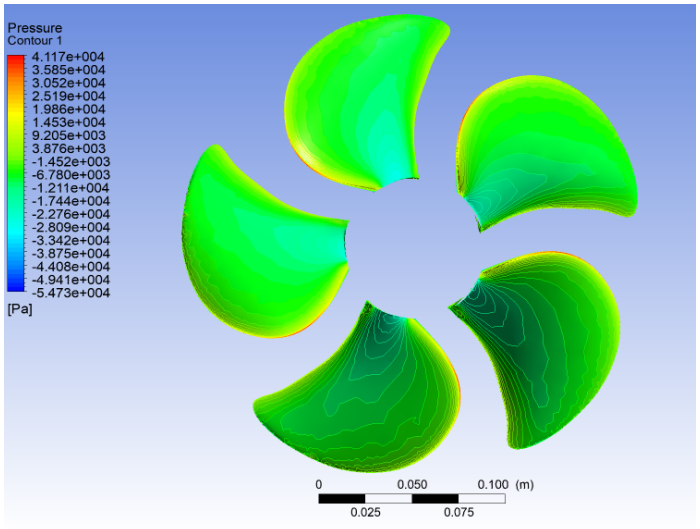

Figure 7 Pressure distribution on the face of propeller for S=0g/kg

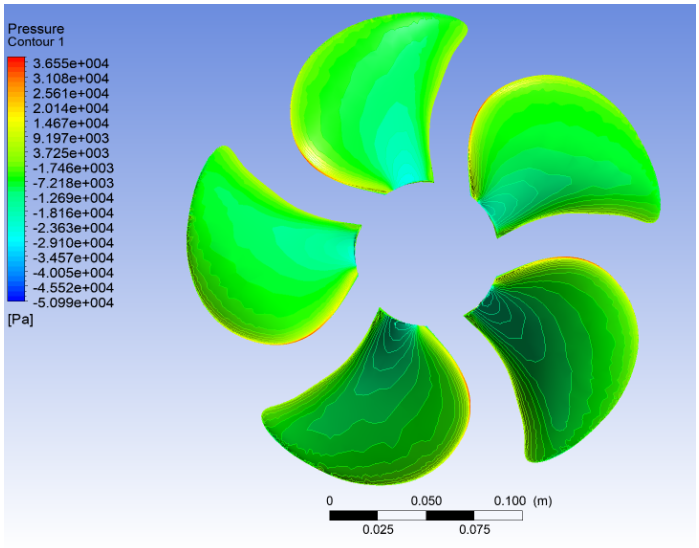

Figure 8 Pressure distribution on the face of propeller for S=100g/kg

5. CONCLUSION

The k-ω sst model was used to establish a numerical model for a five-bladed marine propeller through CFD simulation; the Fluent solver was employed. It was determined that a mesh with $4.6x10^6$ elements would provide the best balance between calculation speed and error stability, so a mesh study was conducted to verify the numerical model. By comparing numerical results with experimental data for the torque, thrust, and efficiency coefficients, the model has been validated, and its robustness has been established, making it suitable for investigating other effects, such as those resulting from changes in geometry or flow. From an open-water performance standpoint, this research looked into how salinity affected propeller behaviour. It was observed that as salinity rose, the overall efficiency of the propeller dropped. Despite the boost in thrust, efficiency decreased for the salinity increases because the propeller needed more torque to rotate in response to the denser flow. As the effect of salinity is readily apparent at low advance ratios, the disparity between thrusts and torques becomes especially pronounced. For larger advance ratios, the difference between the coefficients decreases and they become closer to one another. As a result, the effect of salinity is most significant when the propeller is operating at low speeds and is much less significant when the propeller is working at higher speeds.

References

[1] Boucetta D and Imine O 2016 Numerical Simulation of the Flow around Marine Propeller Series 6 55–61.
[2] Tu T N 2019 Numerical simulation of propeller open water characteristics using RANSE method *Alexandria Eng*.
[3] Prakash.M.N S and R. Nath D 2012 A Computational Method for Determination of Open Water Performance of a Marine Propeller.
[4] Sun W yu and Huang G fu 2019 Integrated lifting line/surface panel method for optimal propeller design with consideration of hub effect J. Hydrodyn. 31 1218–30.
[5] Kowalczyk S 2016 Numerical Simulations of Hydrodynamic Tests Polish Marit. Res. 23 16–22.
[6] Brizzolara S, Villa D and Gaggero S 2007 A systematic comparison between RANS and Panel Methods for Propeller Analysis.
[7] Sikirica A, Carija Z, Kranjcevic L and Lucin I 2019 Grid type and turbulence model influence on propeller characteristics prediction *J. Mar. Sci. Eng.* 7.
[8] Morgut M and Nobile E 2012 Influence of grid type and turbulence model on the numerical prediction of the flow around marine propellers working in uniform inflow *Ocean Eng.* 42 26–34.
[9] Sharqawy M H, V J H L and Zubair S M 2010 Thermophysical properties of seawater : A review of existing correlations and data Thermophysical properties of seawater : a review of existing correlations and data.
[10] Boyd, C., 1998. Pond aeration systems. *Aquacult. Eng.* 18, 9–40.
[11] U Barkmann, H-J Heinke, L Lubke 2011 Potsdam Propeller Test Case (PPTC) Proceeding of the Second International Symposium on Marine Propulsors-smp'11.
[12] Ghassemi H 2009 The E ect of Wake Flow and Skew Angle on the Ship Propeller Performance.
[13] Francesco F Stefano G 2021 Pre-swirl stators design using a coupled BEM-RANSE approach *Ocean Engineering* Volume 222.
[14] Peng H, Qiu W and Ni S 2013 Effect of turbulence models on RANS computation of propeller vortex flow Ocean Eng. 72 304–17.